

Influence of Bead Width and Layer Time on the Interlayer Bonding of Large-Format Printed Polymer Composites

Tyler Corum¹, Maximilian Heres², Jeff Foote², Chad Duty^{1,3}

¹ Mechanical and Aerospace Engineering Department

University of Tennessee

Knoxville, TN

² Loci Robotics, Inc.

Knoxville, TN

³ Manufacturing Science Division

Oak Ridge National Laboratory

Oak Ridge, TN

ABSTRACT

The bonding between printed layers in large-format additive manufacturing (LFAM) is important both for part integrity and to maximize loading potential for specific applications. This study printed multiple parts using LFAM with varied inputs for bead width and layer time to better understand the influence of bead width and layer time on the interlayer strength of LFAM parts. A 2D heat transfer model was developed to determine how the natural cooling of the printed extrudate influences layer bonding. The resulting interlayer strength of each part was measured using flexural testing to understand the bond between printed layers. Results from this work showed a rapid decrease in interlayer bonding for each part once layer time exceeded the time required for the extrudate to cool below glass transition temperature.

1. INTRODUCTION

Large-format additive manufacturing (LFAM) is a process that allows the extrusion of large complex geometries in a layer-by-layer format by using single screw material extrusion [1–3]. This process uses pelletized thermoplastic feedstock in a heated barrel to melt material to a printable state and deposit the extruded bead onto either the print bed or on top of a previously deposited bead. Once deposited, each bead cools naturally until a new hotter bead is deposited upon its top surface and introduces conductive heating. The manner in which these hot thermoplastic beads are deposited influence the bonding between printed layers [4]. Poor bonding between layers can lead to delamination and/or an overall weaker final part [4–7].

This work served as a follow-up study for [8] to investigate the influence of layer time on the interlayer bond strength via the natural cooling of printed beads. Glass transition temperature (T_g) is a material property that has been found by previous studies to impact layer bonding due to a

molecular change that occurs in the material [6,7]. The aim of this study was to understand how bead width and layer time influenced degree of layer bonding by determining the time required for the extrudate to cool to glass transition temperature.

2. MATERIALS AND METHODS

Single bead thick walls spanning only the deposition (x-) and build (z-) direction (referred to as XZ walls) were printed via LFAM at different bead widths and layer times to understand how thermal mass and layer time influenced layer bonding. The XZ walls used in this study were printed using the LOCI-One print system with pelletized 20% by weight carbon fiber reinforced acrylonitrile butadiene styrene (CF-ABS) feedstock in either a small, medium, or large bead width configuration as shown in Figure 1. The print parameters used in this work were identical to [8] with a specific focus on layer time (either 60 seconds, 120 seconds, or 240 seconds) and bead width (either small, medium, or large). Each single bead wall was printed 100 mm high using a 5 mm layer height and a 5 mm diameter nozzle. To understand impacts of layer time on bond strength, a thermal model was developed using SolidWorks to determine time required to cool to T_g . Interlayer bond strength was measured using 4-point bend testing.

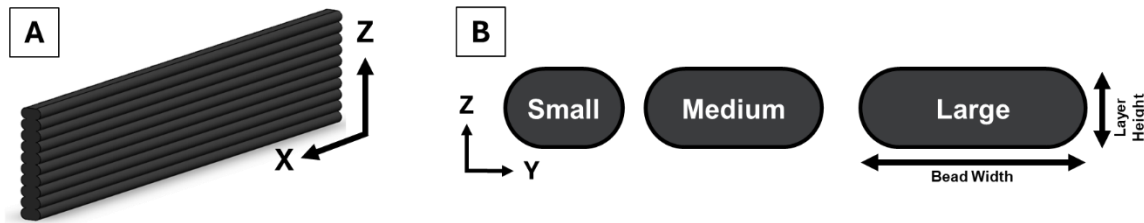


Figure 1. The XZ walls (A) were printed using either a small, medium, or large bead width (B).

2.1 Transient Heat Transfer Model

A 2D heat transfer model was developed using SolidWorks to understand the time required for an extruded bead of CF-ABS to cool from deposition temperature to $T_g = 110\text{ }^\circ\text{C}$. This was accomplished by modeling a representative bead based on average bead width for the small (7.74 mm), medium (10.68 mm), and large (13.99 mm) bead of each sample set from [8] as well as a layer height of 5 mm. The extruded length for the model was set to 1 mm although the extruded length was arbitrary given that this was a 2D model. Material properties for the CF-ABS used in the model were input according to findings for a similar material from [4,9]. This thermal model was defined as a transient simulation that spanned 300 seconds across 2 second intervals. The initial temperature of the printed bead was set as the deposition temperature ($T_{dep} = 250\text{ }^\circ\text{C}$) and the mechanisms of heat transfer for this model were conduction (\dot{q}_{cond}), convection (\dot{q}_{conv}), and radiation (\dot{q}_{rad}) as shown in Figure 2. The conduction boundary condition was imposed on the bottom surface of the bead to account for energy loss to the previously deposited bead by setting the temperature of the bottom surface to T_g . Both convection and radiation were applied to the outer edges of the bead profile excluding the bottom surface. Constants used for heat transfer inputs are defined in Table 1. The mesh was created for each bead using a solid high-quality mesh and

solved using a blended curvature-based algorithm in SolidWorks. The maximum size of each triangular element with the mesh was set to 0.32 mm based on a sensitivity analysis of stable results. To record temperatures at the surface of interest (where the next bead would be deposited), a probe feature was used to collect the temperature over time from each node that comprised the top surface of the bead. The temperatures of these surface nodes were averaged at each time step to determine the average surface temperature of the printed bead for each 2 seconds time step throughout the 300 second simulation.

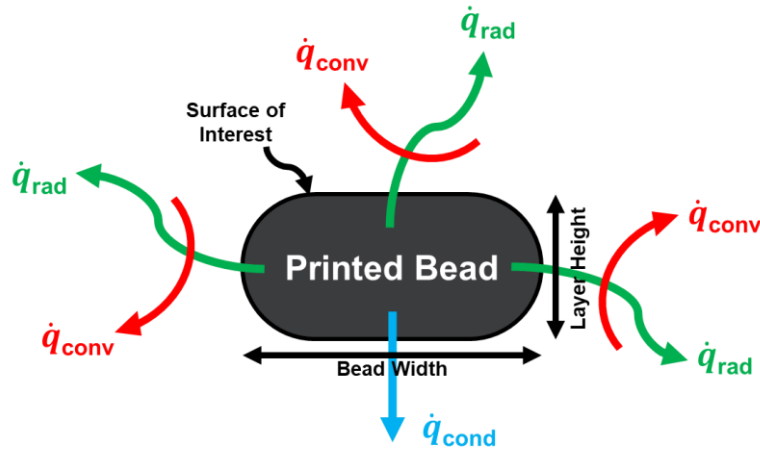


Figure 2. Mechanisms of heat transfer acting on the printed bead during the thermal simulation.

Table 1. Definitions for the heat transfer equations.

Variable	Value	Units	Reference
Natural Convection Coefficient, h	8.5	W/m ²	[4]
Emissivity, ϵ	0.87	---	[4]
Ambient Temperature, T_{∞}	25	°C	---
Initial Temperature, T_i	250	°C	---

2.2 Mechanical Testing

To measure the strength between layers of the printed part (bond strength), 4-point bend (4-pt) test was performed. The XZ walls were face milled on both sides, so the center 3 mm remained once machining was complete. Four specimens from each sample were extracted based on Figure 3 with final dimensions 3 mm x 12.7 mm x 70 mm according to Procedure A of ASTM D6272 [10]. All 4-pt tests were performed using an Instron 5567 load frame, a 30 kN load cell with load span of one third the support span length, and a clip-on extensometer to record displacement during loading. The cross head speed was set to 1.42 mm/min, and the support span was 48 mm for all tests. Each specimen was oriented in the load frame according to Figure 4 so the recorded strength was representative of the bond strength with reduced influence from x-direction.

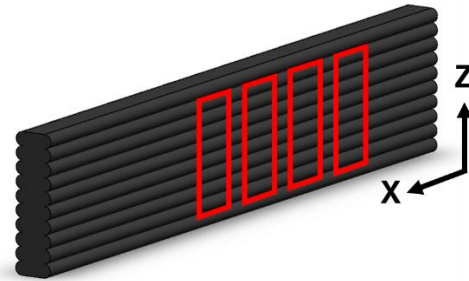


Figure 3. Sampling used for each XZ wall.

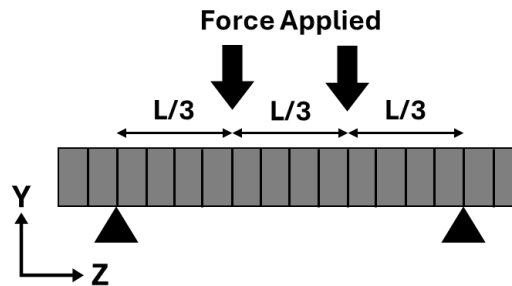


Figure 4. The approach used in this study for measuring bond strength.

3. EXPERIMENTAL RESULTS AND DISCUSSION

3.1 Thermal Cooling

Thermal cooling profiles for each representative bead (b_n) width are shown in Figure 5 for the time step at which they each cooled below T_g . From conduction heat transfer, there is an evident loss of energy to the previously extruded bead (b_{n-1}) for each profile as shown by the green region at the bottom surface for each. This energy loss to b_{n-1} due to condition appeared to increase with larger bead width. Both the convection and radiation boundary conditions clearly show a concentric isothermal profile from the outside of the bead to the center due to energy escaping from the bead to the surrounding air. The area occupied by the isothermal profile varied with increased bead width with primary energy loss moving from the corners of the bead towards the outer edges along the y-direction as width increased. There was also an evident “hot core” at the center of each bead that became wider as bead width increased. These results were encouraging as a simple way to simulate the natural cooling of a deposited extrudate based on inputs from print material and bead geometry.

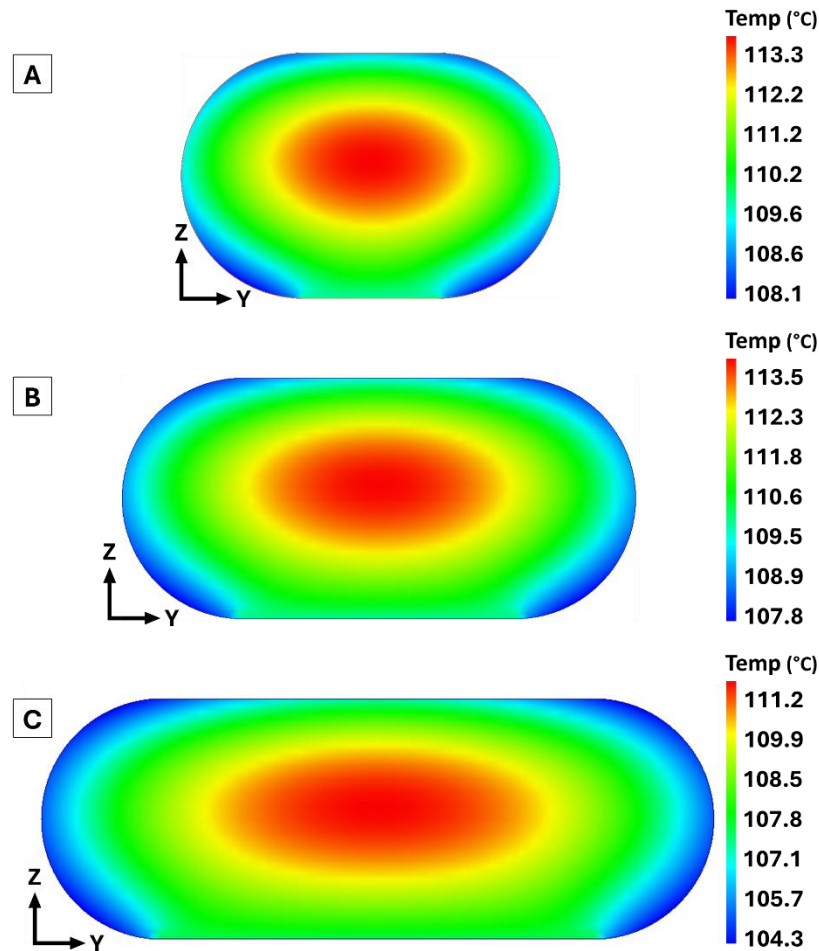


Figure 5. Cooling profiles for the small (A), medium (B), and large (C) representative beads representative beads.

The average temperature for each surface of interest was recorded over time and plotted in Figure 6A for each representative bead with T_g identified as a black dotted line. The enlarged region of the chart (Figure 6B) specifically shows how the different bead widths cooled below T_g . The plot showed an exponential decrease in temperature for each simulated bead. The small, medium, and large bead required 118 seconds, 124 seconds, and 128 seconds, respectively, to cool to T_g . These results suggest that the increased bead width did not drastically increase cooling time at the surface of interest since time values were within 8% of each other. With increased width, the extrudate required more time to cool as expected due to the larger thermal mass.

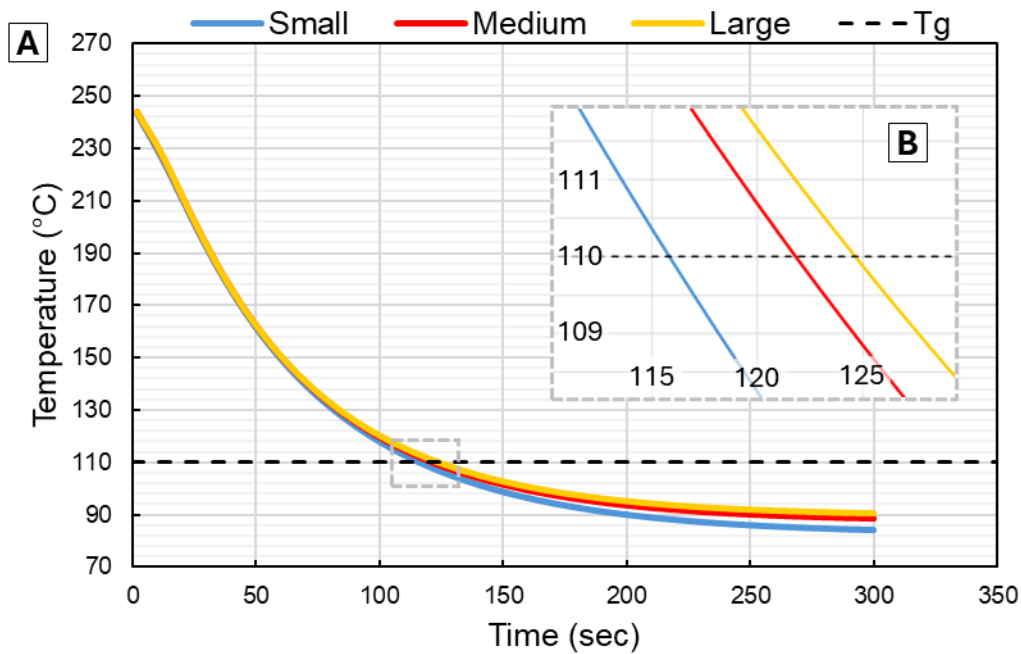


Figure 6. Cooling over time for the small, medium, and large representative bead (A). A specific enlarged region of the chart (B) shows specifically when the different bead widths cooled below glass transition temperature.

3.2 Layer Bonding

The resulting bond strength across increased layer time is shown in Figure 7 with the time required for each bead width to reach T_g represented by the dotted lines. Initially the bond strength ranged between 40 to 50 MPa for each bead deposited using the 60 second layer time, however, once layer time exceeded the time required to cool to T_g , there was a clear drop in bond strength. For the small bead, there was a clear decrease in strength when the layer time was set to 120 seconds and exceeded the 118 seconds required for the extrudate to cool below T_g . For the medium (achieved T_g in 124 seconds) and large (achieved T_g in 128 seconds) beads, the strength was approximately the same from 60 seconds to 120 seconds since the layer was deposited before the bead achieved T_g . However, the medium and large bead widths saw a drastic decrease in bonding when layer time was set to 240 seconds due to layer time exceeding time required to cool to T_g . Strength ranged from 10 to 25 MPa for each bead deposited at the 240 second layer which signified a clear influence of bead cooling on layer bonding. If the time required to deposit a new bead exceeds the time required for the bead to cool to T_g , the strength between layers will decrease.

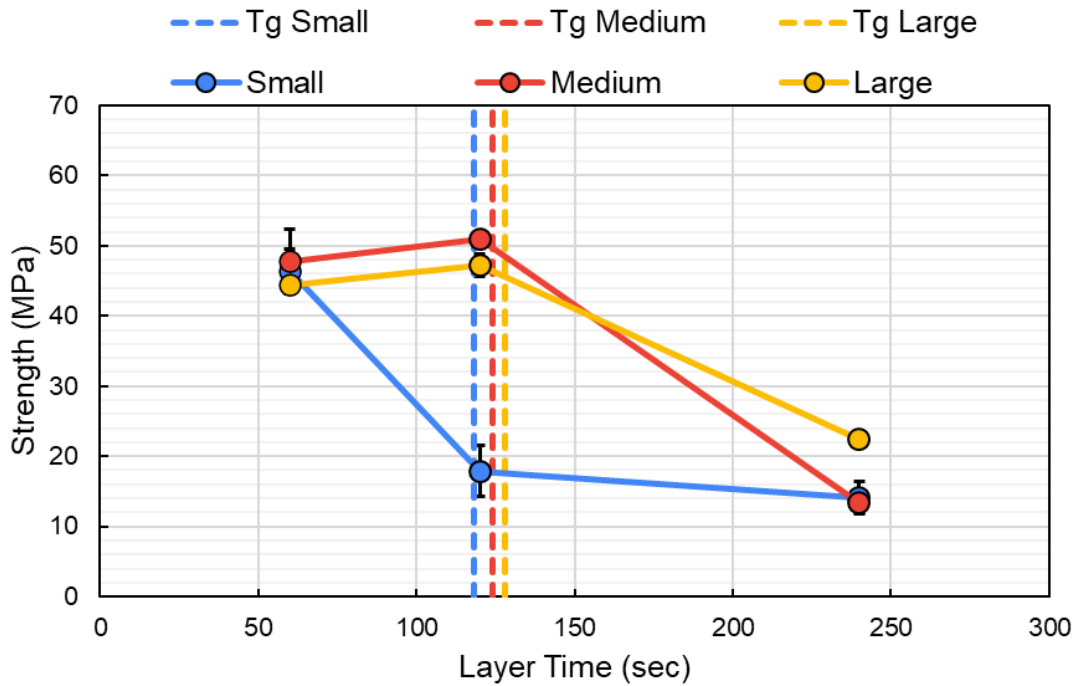


Figure 7. Bond strength as a result of increased layer time with time required for the extrudate to cool to T_g shown as dotted lines.

4. CONCLUSIONS

The goal of this study was to relate the influence of layer time on interlayer strength. To accomplish this, parts were printed using either a small, medium, or large bead width and a layer time of 60 seconds, 120 seconds, and 240 seconds. A thermal model was developed using SolidWorks to understand the time required by a small, medium, and large bead to cool to T_g (110 °C). Bond strength was tested using 4-pt to determine the interface strength between printed layers based on the bead width and layer time used during printing. The thermal simulation was used to determine that the small, medium, and large bead widths required 118 seconds, 124 seconds, and 128 seconds, respectively, to cool to T_g . Strength data revealed a loss of strength for each bead width once the layer time exceeded this time needed to cool to T_g . Understanding this relationship between layer time, bond strength, and thermal cooling is important so that the strength of LFAM strong parts will not be limited by poor layer times during the deposition process.

5. ACKNOWLEDGEMENTS

This research was funded by the Southeastern Advanced Machine Tools Network (SEAMTN) through the U.S. Department of Defense, Defense Manufacturing Community Support Program, under Grant No. MCS1940-21-01. This study was also sponsored by the U.S. Department of Energy, Office of Energy Efficiency and Renewable Energy, Advanced Manufacturing Office, under contract DE-AC05-00OR22725 with UT- Battelle, LLC and partially supported by the

National Science Foundation under Grant No. 2055529. The authors would like to thank the following groups for their assistance in this study: the Manufacturing Core at the University of Tennessee for machining the printed material and Dr. David Harper with the Center for Renewable Carbon for assistance with 4-point bend testing.

6. REFERENCES

- [1] C.E. Duty, V. Kunc, B. Compton, B. Post, D. Erdman, R. Smith, R. Lind, P. Lloyd, L. Love, Structure and mechanical behavior of Big Area Additive Manufacturing (BAAM) materials, *Rapid Prototyp. J.* 23 (2017) 181–189. <https://doi.org/10.1108/RPJ-12-2015-0183>.
- [2] C.E. Duty, T. Drye, A. Franc, Material Development for Tooling Applications Using Big Area Additive Manufacturing (BAAM), 2015. <https://doi.org/10.2172/1209207>.
- [3] B. Post, B. Richardson, R. Lind, L.J. Love, P. Lloyd, V. Kunc, B.J. Rhyne, A. Roschli, J. Hannan, S. Nolet, K. Veloso, P. Kurup, T. Remo, D. Jenne, BIG AREA ADDITIVE MANUFACTURING APPLICATION IN WIND TURBINE MOLDS, in: *Proc. 28th Annu. Int. Solid Free. Fabr. Symp. – Addit. Manuf. Conf.*, 2017: p. 17. <http://dx.doi.org/10.26153/tsw/16964>.
- [4] B.G. Compton, B.K. Post, C.E. Duty, L. Love, V. Kunc, Thermal analysis of additive manufacturing of large-scale thermoplastic polymer composites, *Addit. Manuf.* 17 (2017) 77–86. <https://doi.org/10.1016/j.addma.2017.07.006>.
- [5] V. Kishore, C. Ajinjeru, A. Nycz, B. Post, J. Lindahl, V. Kunc, C. Duty, Infrared preheating to improve interlayer strength of big area additive manufacturing (BAAM) components, *Addit. Manuf.* 14 (2017) 7–12. <https://doi.org/10.1016/j.addma.2016.11.008>.
- [6] J.E. Seppala, S. Hoon Han, K.E. Hillgartner, C.S. Davis, K.B. Migler, Weld formation during material extrusion additive manufacturing, *Soft Matter* 13 (2017) 6761–6769. <https://doi.org/10.1039/C7SM00950J>.
- [7] Q. Sun, G.M. Rizvi, C.T. Bellehumeur, P. Gu, Effect of processing conditions on the bonding quality of FDM polymer filaments, *Rapid Prototyp. J.* 14 (2008) 72–80. <https://doi.org/10.1108/13552540810862028>.
- [8] T. Corum, J. O’Connell, M. Heres, J. Foote, C. Duty, CHARACTERIZING THERMOMECHANICAL PROPERTIES OF LARGE-FORMAT PRINTED COMPOSITE POLYMER STRUCTURES, in: *Proc. 34th Annu. Int. SOLID Free. Fabr. Symp. 2023 – Addit. Manuf. Conf.*, Austin, TX, 2023: p. 9. <https://doi.org/10.26153/tsw/51079>.
- [9] A.A. Hassen, R.B. Dinwiddie, S. Kim, H.L. Tekinap, V. Kumar, J. Lindahl, P. Yeole, C. Duty, U. Vaidya, H. Wang, V. Kunc, Anisotropic thermal behavior of extrusion-based large scale additively manufactured carbon-fiber reinforced thermoplastic structures, *Polym. Compos.* 43 (2022) 3678–3690. <https://doi.org/10.1002/pc.26645>.
- [10] D20 Committee, Test Method for Flexural Properties of Unreinforced and Reinforced Plastics and Electrical Insulating Materials by Four-Point Bending, ASTM International, n.d. <https://doi.org/10.1520/D6272-17E01>.